ELSEVIER

Journal of Structural Geology 26 (2004) 1693–1705

JOURNAL OF STRUCTURAL GEOLOGY

www.elsevier.com/locate/jsg

Composite flow laws for crystalline materials with log-normally distributed grain size: theory and application to olivine

J.H. Ter Heege*, J.H.P. De Bresser, C.J. Spiers

High Pressure and Temperature Laboratory, Faculty of Earth Sciences, Utrecht University, PO Box 80021, 3508 TA Utrecht, The Netherlands

Received 13 February 2003; received in revised form 27 December 2003; accepted 18 January 2004

Available online 9 April 2004

Abstract

Conventional steady-state flow laws describing combined grain size insensitive dislocation creep and grain size sensitive diffusion creep incorporate grain size as a single (mean) value. However, rocks exhibit distributed grain size and variations in the shape of the distribution, such as its width, will accordingly affect rheological behavior. To evaluate this effect, we have derived composite dislocation–diffusion flow laws describing upper and lower bounds on the rate of deformation of materials showing a grain size distribution of the commonly observed log-normal type. The upper and lower bound flow laws obtained allow systematic investigation of the influence of the grain size distribution parameters, i.e. the median and standard deviation, on composite rheology. The results demonstrate major effects of distribution width as well as median value. Application to polycrystalline olivine, deforming by Coble creep and power law dislocation creep, reveals significant implications for interpreting deformation experiments and modeling flow in the Earth's mantle. The flow laws also provide an improved basis for modeling the deformation of rocks during geological processes in the crust and mantle.

Keywords: Rheology; Flow laws; Grain size distribution; Olivine

1. Introduction

In formulating steady state flow laws for polycrystalline materials, the microstructure of the material is usually regarded as fixed, with a constant, single-valued (mean) grain size (Tsenn and Carter, 1987; Rutter and Brodie, 1988; Kohlstedt et al., 1995). However, rocks invariably exhibit a grain size distribution (Kretz, 1966; Ranalli, 1984; Michibayashi, 1993; Newman, 1994; Miralles et al., 2000; Molli et al., 2000; Dijkstra et al., 2002). Small grains within such a distribution may deform by grain size sensitive mechanisms such as diffusion creep, while larger grains may deform by grain size insensitive dislocation creep. This means that differences in grain size distribution parameters between otherwise similar rock materials or samples could have major effects on rheology (Heilbronner and Bruhn, 1998). To evaluate such effects, a composite grain size sensitive (GSS) and grain size insensitive (GSI) rate equation is needed, in which the grain size distribution parameters explicitly determine the relative (volumetric) contributions of GSI versus GSS mechanisms (Raj and Ghosh, 1981; Freeman and Ferguson, 1986; Wang, 1994).

Raj and Ghosh (1981) used both analytical and numerical methods to investigate the effect of varying bimodal and simple multimodal grain size distributions on the composite GSS–GSI rheology of polycrystalline materials, assuming uniform strain rate in all grains. Wang (1994) later extended the analysis of Raj and Ghosh (1981) to investigate the effect of varying bimodal grain size distributions on apparent power law parameters, such as the stress exponent (n), grain size exponent and activation energy, for the cases of uniform strain rate and uniform stress. Both studies demonstrated marked effects of varying grain size distribution. However, rock materials usually exhibit continuous, unimodal grain size distributions rather than (discrete) bimodal or multimodal distributions. Using numerical methods, Freeman and Ferguson (1986) investigated the effects of variations in geologically realistic grain size distributions, namely discrete log-normal and bimodal distributions, again considering both uniform strain rate and uniform stress cases. They showed that for distributions

* Corresponding author. Now at: Institute for Geology, Mineralogy and Geophysics, Ruhr-University Bochum, Germany. Tel.: +49-234-3225909; fax: +49-234-5214181.

E-mail address: jan.terheege@ruhr-uni-bochum.de (J.H. Ter Heege).

0191-8141/$ - see front matter © 2004 Elsevier Ltd. All rights reserved.
doi:10.1016/j.jsg.2004.01.008

with similar mean grain size, variations in distribution type and width have substantial effects on flow strength and on the width of the zone, in stress–temperature space, where both GSS and GSI mechanisms contribute significantly to the overall strain rate.

In the present paper, we derive combined GSS–GSI creep equations for materials showing a continuous grain size distribution of the log-normal type commonly observed in rocks (Kretz, 1966; Ranalli, 1984; Michibayashi, 1993; Miralles et al., 2000; Dijkstra et al., 2002). The grain size distribution appears explicitly in the creep equation in the form of the median grain size and standard deviation of the distribution of grain size, represented by the volume-equivalent diameter. Composite creep equations are derived, assuming either the applied stress or strain rate to be homogeneous throughout the material. These equations, respectively, describe lower and upper bounds for the rate of deformation, in a manner analogous to the Reuss and Voight bounds for elastic behavior (Hashin, 1964; Hill, 1965; Tullis et al., 1991). After a general derivation, we focus on Coble creep and dislocation creep. Though several approximations are made, our flow laws possess the advantage of algebraic form allowing systematic investigation of the effect of the distribution parameters on rheology. In addition, they can be applied to any material deforming under experimental or natural conditions in more or less the same way as conventional flow laws, provided grain size is spatially non-correlated (i.e. the material does not form weak interconnected layers of small grains or load bearing frameworks of large grains, cf. Handy, 1990), the grain size distribution is of a log-normal type and the distribution parameters have been analyzed. We have limited ourselves to lognormal distributions, but other types of grain size distributions can be modeled following the same procedure as presented in this study.

In addition to deriving composite flow laws for distributed grain size, we apply our flow laws to describe the rheological behavior of polycrystalline olivine, using flow law parameters from Karato et al. (1986). The results show that varying the standard deviation of the grain size distribution at constant median grain size and temperature can yield order of magnitude changes in strain rate, as well as switches between dislocation and diffusion dominated creep with associated rheological softening or hardening. The olivine example illustrates the importance of incorporating grain size distributions in the calibration and application of flow laws.

2. Model development

Our model addresses a single-phase polycrystalline material, with spatially non-correlated, log-normally distributed grain size, undergoing steady state, axi-symmetric deformation by GSS and GSI mechanisms, operating as independent, parallel-concurrent processes (Poirier, 1985, p. 79). In the latter stages of our treatment, we restrict attention to Coble creep (Coble, 1963), and power law, recovery-controlled dislocation creep (Weertman, 1968; Frost and Ashby, 1982, p. 12). The Coble creep mechanism considered here occurs by solid-state diffusion along grain boundaries accommodated by grain boundary sliding. The analysis can easily be modified to incorporate other GSS mechanisms, such as solid state diffusion through the crystal lattice accommodated by grain boundary sliding (Nabarro, 1948; Herring, 1950), grain boundary sliding with grain neighbor switching accommodated by solid state diffusion (Ashby and Verall, 1973) or dislocation processes (e.g. Mukherjee, 1975), or other GSI mechanisms (e.g., Poirier, 1985, pp. 94–124). We follow a three-step approach. In the first step, a composite diffusion–dislocation flow law for a single-valued grain size (Fig. 1a and b) is obtained (Frost and Ashby, 1982; Poirier, 1985). In the second step, composite flow laws for discrete grain size distributions (Fig. 1c and d) are derived, making end member assumptions that stress or strain rate is distributed homogeneously throughout the material. The average bulk strain rate or

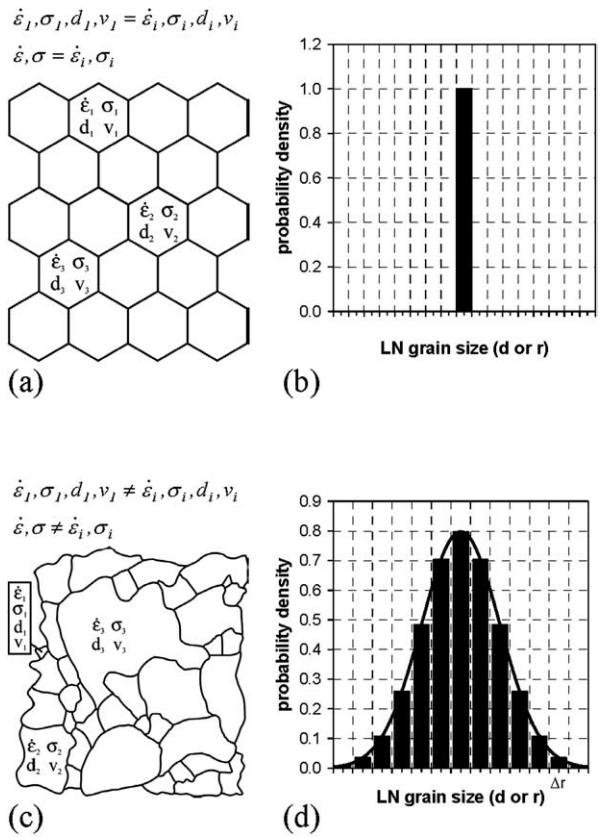

Fig. 1. Schematic diagrams of polycrystalline aggregates with a single-valued grain size (a) and a distributed grain size (c), plus corresponding probability density distributions (b) and (d). For the distributed grain size (c), discrete and continuous log-normal probability density distributions are shown (d). Note that the local strain rate $\dot{\epsilon}_i$, stress σ_i and grain size d_i vary from grain to grain (interval to interval) in (c) but are uniform in (a). Grain size distributions can be viewed as distributions of grain diameter d or radius $r = d/2$.

Table 1
List of symbols used with explanation and S.I. units

Symbol[a]	Description, expression [units]
$A(T)$, $B(T)$	Temperature dependent material parameter diffusion creep [$m^m\ s^{-1}$], dislocation creep [s^{-1}]
A	Rate constant
b	Magnitude of Burgers' Vector [m]
C	Normalized factor containing material parameters, distribution parameters and temperature
d	Grain size (diameter), $d = 2r$ [m]
dr	Grain size interval in a continuous distribution [m]
D_0, D	(Pre-exponential) diffusion coefficient[b], $D = D_0 \exp\left[\frac{-Q}{RT}\right]$, $D_{\text{diff}} = D_v + \frac{\pi\delta}{b} D_b$ [$m^2\ s^{-1}$]
$F(\bar{\sigma}^*_{\dot{\epsilon}}, \phi, n, m)$	Empirical fitted function
i, j	Grain size class number, total number of grain size classes in a discrete distribution
k	Boltzmann's constant [$J\ K^{-1}$]
K	Shape factor, $K = \frac{4}{3}\pi$ for spherical grains
m, n	Grain size, power law stress exponent
N_t	Total number of grains in a polycrystalline material
p, q	Constants
Q	Activation energy [$J\ mol^{-1}$]
r	Grain radius, $r = \frac{1}{2}d$ [m]
R	Gas constant [$J\ mol^{-1}\ K^{-1}$]
S	Normalized strain rate
T	Absolute temperature [K]
v	Volume fraction
V_t	Total volume of material [m^3]
X	Grain size (distribution) term [m]
z	Substitution variable
α, β, γ	Empirical constants in function $F(\bar{\sigma}^*_{\dot{\epsilon}}, \phi, n, m)$
δ	Diffusive thickness of a grain boundary *[m]*
Δ	Error in strain rate between $\dot{\epsilon}^{\text{rough}}_{\dot{\epsilon}}$ and $\dot{\epsilon}^{\text{true}}_{\dot{\epsilon}}$ [%]
Δr	Width of a grain size class in a discrete distribution [m]
$\dot{\epsilon}$	Strain rate [s^{-1}]
ϕ	Standard deviation of a log-normal grain size distribution
μ	Shear modulus[b] [Pa]
π	Constant pi
$\bar{\sigma}$, σ	(Normalized) flow stress, $\bar{\sigma} = (\sigma/\mu)$, $\bar{\sigma}^*_{\sigma} = \bar{\sigma}_{\sigma}/\bar{\sigma}^{\text{int}}_{\sigma}$ [Pa]
$\Lambda(r)$	Probability density function of grains in a continuous distribution

[a] Sub- or superscript 'diff': for pure diffusion creep (single mechanism), e.g. A_{diff}, D_{diff}, $D_{0\text{diff}}$, Q_{diff}, $\dot{\epsilon}_{\text{diff}}$, $\bar{\sigma}_{\text{diff}}$, $\dot{\epsilon}^{\text{diff}}_{\dot{\epsilon}}$; sub- or superscript 'disl': for pure dislocation creep (single mechanism), e.g. A_{disl}, D_{disl}, $D_{0\text{disl}}$, Q_{disl}, $\dot{\epsilon}_{\text{disl}}$, $\bar{\sigma}^{\text{disl}}_{\dot{\epsilon}}$; subscript 'b': grain boundary diffusion, e.g. D_b, Q_b; subscript 'v': lattice diffusion, e.g. D_v, Q_v; Subscript '*i*': for grains in class *i* of a discrete distribution, e.g. $d_i, r_i, v_i, \dot{\epsilon}_i, \sigma_i, \bar{\sigma}_i$; subscript '*j*': for grains in the last class of a discrete distribution, e.g. $v_j\ \dot{\epsilon}_j, \bar{\sigma}_j$; subscript 'med': median of a continuous log-normal distribution, e.g. d_{med}, r_{med}; subscript '$\dot{\epsilon}$': for a continuous log-normal distribution assuming uniform strain rate, e.g. $\dot{\epsilon}_{\dot{\epsilon}}$, $\sigma_{\dot{\epsilon}}$, $\bar{\sigma}_{\dot{\epsilon}}$; subscript '$\sigma$': for a continuous log-normal distribution assuming uniform stress, e.g. $\dot{\epsilon}_{\sigma}$, σ_{σ}, $\bar{\sigma}_{\sigma}$; superscript 'rough', 'approx', 'true': rough, approximated, true value, e.g. $\dot{\epsilon}^{\text{rough}}_{\dot{\epsilon}}$, $\dot{\epsilon}^{\text{approx}}_{\dot{\epsilon}}$, $\dot{\epsilon}^{\text{true}}_{\dot{\epsilon}}$; superscript 'int': at the intersection between pure diffusion and pure dislocation creep (single mechanisms), e.g. $\bar{\sigma}^{\text{int}}_{\dot{\epsilon}}$; '$(r)$': for grains of radius *r* in a log-normal distribution, e.g. $\dot{\epsilon}(r)$, $\bar{\sigma}(r)$.

[b] Frost and Ashby (1982).

stress is obtained by summing the values associated with individual grain size classes according to their volume fraction (i.e. by volume averaging) following Raj and Ghosh (1981). In the third step, a continuous log-normal grain size distribution (Aitchison and Brown, 1957) is incorporated into the composite flow law (Fig. 1d). All symbols used in our analysis are defined in Table 1.

2.1. Composite flow law for a single-valued grain size

We use the following theoretical rate equation for diffusion creep of a polycrystalline material characterized by a single-valued grain size d (see Fig. 1a and b):

$$\dot{\epsilon}_{\text{diff}} = \frac{A_{\text{diff}} b D_{\text{diff}} \mu}{kT} \left(\frac{b}{d}\right)^m \left(\frac{\sigma}{\mu}\right) \tag{1}$$

This represents grain boundary sliding accommodated by grain boundary diffusion (called Coble creep hereafter) if $m = 3$ and $D_{\text{diff}} = \pi\delta D_b/b$, or grain boundary sliding accommodated by lattice diffusion (Nabarro–Herring creep) if $m = 2$ and $D_{\text{diff}} = D_v$ (see Table 1). If grain boundary sliding is accommodated by dislocation processes, a nonlinear dependence of strain rate on stress is introduced in Eq. (1), but for simplicity we restrict the derivation to GSS mechanisms that show a linear dependence of strain rate on stress. For power law dislocation creep, we use (Frost and Ashby, 1982, p. 12):

$$\dot{\epsilon}_{\text{disl}} = \frac{A_{\text{disl}} b D_{\text{disl}} \mu}{kT} \left(\frac{\sigma}{\mu}\right)^n \tag{2}$$

Microphysical models for climb-controlled dislocation creep typically predict n-values of 3 or 4.5, and possibly up to 6 (Weertman, 1968). However, other values of n are often found experimentally, and although it is doubtful if Eq. (2) can be applied when $n > 5$, it can conveniently be used to describe the creep rate accurately if $3 \leq n \leq 5$ (Poirier, 1985, p. 111). Since the above GSS and GSI mechanisms contribute independently to the overall strain rate, summation gives the composite flow law:

$$\dot{\epsilon} = \left[\frac{A_{\text{diff}} b D_{\text{diff}} \mu}{kT} \left(\frac{b}{d}\right)^m \left(\frac{\sigma}{\mu}\right)\right] + \left[\frac{A_{\text{disl}} b D_{\text{disl}} \mu}{kT} \left(\frac{\sigma}{\mu}\right)^n\right] \tag{3}$$

2.2. Composite flow law for discrete grain size distributions

Consider a polycrystalline material characterized by a discrete grain size distribution consisting of j grain radius classes, each centered about a radius $r_i = d_i/2$ and of width Δr (Fig. 1c and d). For an individual grain size class in such a distribution, Eq. (3) yields:

$$\dot{\epsilon}_i = \frac{A(T)}{r_i^m} \bar{\sigma}_i + B(T) \bar{\sigma}_i^n \tag{4}$$

where

$$A(T) = \frac{A_{\text{diff}} b^{m+1} D_{\text{diff}} \mu}{2^m kT},$$

$$B(T) = \frac{A_{\text{disl}} b D_{\text{disl}} \mu}{kT}$$

and

$$\bar{\sigma}_i = \frac{\sigma_i}{\mu}$$

In order to derive equations for the overall creep rate of our material, we now make the following assumptions: (i) grain size is spatially non-correlated, i.e. no interconnected weak layers of fine grains or load-bearing frameworks of large grains, analogous to some two phase materials with strong viscosity contrast between the phases, are formed (Handy, 1990), (ii) the morphology of grains does not change between individual classes and (iii) either stress or strain rate is uniform throughout the sample. Together with Eq. (3), assumption (iii) implies that strain rate or stress must vary abruptly from grain to grain according to grain size (Raj and Ghosh, 1981; Freeman and Ferguson, 1986). In real polycrystals, strain compatibility and stress equilibrium are maintained by more continuous stress and strain rate gradients, analogous to the distribution of stress and strain between different phases in polyphase materials (Raj and Ghosh, 1981; Tullis et al., 1991).

If the stress is assumed to be uniform throughout a material with distributed grain size, Eq. (4) requires that the grains in different grain size classes will deform at different rates. We assume that the contribution of each grain size class to the bulk strain rate ($\dot{\epsilon}_\sigma$) is determined by the volume fraction v_i of the grains in that class (Tullis et al., 1991). In other words, the bulk creep rate under given conditions can be obtained by volume-averaging the strain rates as given by Eq. (4) for the individual grain size classes (Raj and Ghosh, 1981; Freeman and Ferguson, 1986), so that

$$\dot{\epsilon}_\sigma = \dot{\epsilon}_1 v_1 + \dot{\epsilon}_2 v_2 + \ldots + \dot{\epsilon}_j v_j = \sum_{i=1}^{i=j} \dot{\epsilon}_i v_i$$

$$= \sum_i \left(\frac{A(T)}{r_i^m} \bar{\sigma}_i + B(T) \bar{\sigma}_i^n \right) v_i \qquad (5a)$$

If the strain rate is assumed to be uniform throughout the material, the normalized bulk stress $\bar{\sigma}_{\dot{\epsilon}}$ can be similarly obtained by volume-averaging the stresses $\bar{\sigma}_i$ for the individual grain size classes given by Eq. (4), so that

$$\bar{\sigma}_{\dot{\epsilon}} = \bar{\sigma}_1 v_1 + \bar{\sigma}_2 v_2 + \ldots + \bar{\sigma}_j v_j = \sum_i \bar{\sigma}_i v_i \qquad (5b)$$

Here, $\bar{\sigma}_i$ is the root of Eq. (4) for each grain size class at the imposed strain rate. Eqs. (5a) and (5b) constitute bulk $\sigma - \dot{\epsilon}$ relations, which can be investigated numerically, as Freeman and Ferguson (1986) did, by inserting v_i values reflecting specific discrete grain size distributions.

2.3. Composite flow laws for a continuous grain size distribution

For continuous distributions, the number of grain size classes $j \to \infty$ and the class interval $dr \to 0$. If an appropriate probability density function $\Lambda(r)$ is chosen to describe the grain radius distribution (cf. Fig. 1d) and the total number of grains in volume V_t is N_t, then the number of grains falling in a radius interval dr of $\Lambda(r)$ is $\Lambda(r)drN_t$. Since the volume of each grain is Kr_i^3 (where K is a shape factor, equal to $4/3\pi$ for spherical grains), the volume fraction of grains falling in the radius interval dr is $(\Lambda(r)drN_tKr^3)/V_t$. For a continuously distributed grain size (Eqs. (5a) and (5b)) can hence be re-written in the form:

$$\dot{\epsilon}_\sigma = \int_0^\infty \dot{\epsilon}(r) \left(\frac{\Lambda(r) N_t K r^3}{V_t} \right) dr \qquad (6a)$$

and

$$\bar{\sigma}_{\dot{\epsilon}} = \int_0^\infty \bar{\sigma}(r) \left(\frac{\Lambda(r) N_t K r^3}{V_t} \right) dr \qquad (6b)$$

In order to evaluate the integrals of Eqs. (6a) and (6b), the distribution of 3-D grain radii in natural rock materials is required. Quantification of 3-D grain size distributions is a difficult task. Except for some studies that determine 3-D grain size distributions from 2-D measurements of linear intercepts or grain area (e.g. Heilbronner and Bruhn, 1998), almost all studies report 2-D grain size distributions. These grain size distributions may take a variety of forms, depending on the relative contribution of the microphysical processes that were involved in producing the microstructure. However, there is evidence that the distribution of 2-D grain size is approximately log-normal in materials that have undergone dynamic recrystallization or grain growth, both in nature (Kretz, 1966; Ranalli, 1984; Michibayashi, 1993; Dijkstra et al., 2002) and experiment (Humphreys and Hatherly, 1996; Post and Tullis, 1999). Although there is some indication that log-normality of distributions is maintained upon conversion from 2-D to 3-D grain size (Schückher, 1968), this cannot be taken as a general rule and 3-D grain size distributions may differ from the 2-D distribution they were derived from (Heilbronner and Bruhn, 1998). It is beyond the scope of this paper to discuss in detail the 2-D to 3-D conversion of grain size and its consequences for the shape of the distribution. For most grain size distributions, the error in strain rate that is introduced by assuming that the 3-D grain size distributions are log-normal will be negligible compared with the error that is introduced if grain size is taken as a single value. More complex distributions may be modeled by introducing more complex descriptions of $\Lambda(r)$ in Eqs. (6a) and (6b). For example multimodal distributions may be represented by adding several log-normal distributions, yielding separate terms for each distribution in the integral of Eqs. (6a) or (6b). In this study, we assume that $\Lambda(r)$ can be described by the standard log-normal probability density distribution:

$$\Lambda(r) = \frac{1}{\sqrt{2\pi}\phi} \frac{1}{r} \exp\left[- \frac{(\ln r - \ln r_{med})^2}{2\phi^2} \right] \qquad (7)$$

for which the area beneath the curve is unity, i.e. $\int_0^\infty \Lambda(r)\,\mathrm{d}r = 1$ (Aitchison and Brown, 1957). The parameters characterizing the distribution are the median grain radius (r_{med}) and standard deviation (ϕ). For this distribution, the total volume of grains can be expressed as:

$$V_{\mathrm{t}} = \int_0^\infty N_{\mathrm{t}} K r^3 \Lambda(r)\mathrm{d}r = \frac{N_{\mathrm{t}}K}{\sqrt{2\pi}} \int_0^\infty \frac{r^2}{\phi} \exp\left[-\frac{(\ln r - \ln r_{\mathrm{med}})^2}{2\phi^2} \right] \mathrm{d}r \quad (8)$$

Putting $z = (\ln r - \ln r_{\mathrm{med}})/\phi$ then leads to:

$$V_{\mathrm{t}} = \frac{N_{\mathrm{t}}K}{\sqrt{2\pi}} r_{\mathrm{med}}^3 \int_{-\infty}^\infty \exp\left[-\frac{1}{2}z^2 + 3\phi z \right] \mathrm{d}z \quad (9)$$

which, using the standard integral given by Gradshteyn and Ryzhik (1980):

$$\int_{-\infty}^\infty \exp\left[-p^2 z^2 \pm qz \right] \mathrm{d}z = \frac{\sqrt{\pi}}{p} \exp\left[\frac{q^2}{4p^2} \right] \text{ for } p > 0 \quad (10)$$

reduces to

$$V_{\mathrm{t}} = N_{\mathrm{t}} K r_{\mathrm{med}}^3 \exp\left[\frac{9}{2}\phi^2 \right] \quad (11)$$

2.3.1. Flow law assuming homogeneous stress

The overall creep rate of a polycrystalline material with a log-normal grain size distribution, for the case that the stress $\bar{\sigma} = \sigma/\mu$ is uniform (i.e. constant) throughout the aggregate, can now be found by putting Eqs. (11) and (7) and the expression for $\dot{\epsilon}(r)$ embodied by Eq. (4) into Eq. (6a). This yields

$$\dot{\epsilon}_\sigma = \frac{1}{\sqrt{2\pi}\phi \exp[\frac{9}{2}\phi^2] r_{\mathrm{med}}^3} \int_0^\infty (A(T) r^{2-m} \bar{\sigma}_\sigma + B(T) r^2 \bar{\sigma}_\sigma^n) \times \left(\exp\left[-\frac{(\ln r - \ln r_{\mathrm{med}})^2}{2\phi^2} \right] \right) \mathrm{d}r \quad (12)$$

which, using the aforementioned substitution $z = (\ln r - \ln r_{\mathrm{med}})/\phi$, and standard integral (10) reduces to

$$\dot{\epsilon}_\sigma = \left[\frac{A_{\mathrm{diff}} b D_{\mathrm{diff}} \mu}{kT} \left(\frac{b}{\exp[(3 - \frac{1}{2}m)\phi^2] d_{\mathrm{med}}} \right)^m \left(\frac{\sigma_\sigma}{\mu} \right) \right] + \left[\frac{A_{\mathrm{disl}} b D_{\mathrm{disl}} \mu}{kT} \left(\frac{\sigma_\sigma}{\mu} \right)^n \right] \quad (13)$$

Note that the first term on the right of this equation gives the strain rate (flow law) for diffusion creep in materials with a log-normal grain size distribution, assuming homogeneous stress (cf. Eq. (1)).

2.3.2. Flow law assuming homogeneous strain rate

The derivation of a flow law under the assumption that the strain rate is uniform throughout a polycrystalline material is more difficult, since it requires finding an expression for $\bar{\sigma} = \bar{\sigma}(\dot{\epsilon}, r, T)$ in Eq. (6b), i.e. for the stress in individual grains of radius r ($= d/2$). This is not straightforward as it means solving for $\bar{\sigma} = \sigma/\mu$ in Eq. (3)—an nth-order polynomial in $\bar{\sigma}$ where n is the power law stress exponent taking values between 3 and 5. The problem can be tackled by first evaluating Eq. (6b) separately for dislocation and diffusion creep. An expression for $\bar{\sigma}(\dot{\epsilon}, r, T)$ when deformation takes place by diffusion creep alone in a single grain is given by Eq. (1) as:

$$\bar{\sigma}_{\mathrm{diff}} = \frac{kT\dot{\epsilon}_{\mathrm{diff}}}{A_{\mathrm{diff}} b D_{\mathrm{diff}} \mu} \left(\frac{b}{d} \right)^m = \frac{\dot{\epsilon}_{\mathrm{diff}} r^m}{A(T)} \quad (14)$$

where $d = 2r$ and $A(T)$ is defined as in Eq. (4). Putting Eqs. (7), (11) and (14) into Eq. (6b) and again using our substitution $z = (\ln r - \ln r_{\mathrm{med}})/\phi$ plus standard integral (10), now yields

$$\bar{\sigma}_{\dot{\epsilon}}^{\mathrm{diff}} = \frac{\dot{\epsilon}_{\dot{\epsilon}}^{\mathrm{diff}}}{A(T)\sqrt{2\pi}\phi \exp[\frac{9}{2}\phi^2] r_{\mathrm{med}}^3} \int_0^\infty r^{m+2} \exp\left[-\frac{(\ln r - \ln r_{\mathrm{med}})^2}{2\phi^2} \right] \mathrm{d}r = \frac{(\exp[(3 + \frac{1}{2}m)\phi^2] r_{\mathrm{med}})^m \dot{\epsilon}_{\dot{\epsilon}}^{\mathrm{diff}}}{A(T)} \quad (15)$$

This is the volume averaged stress for a material with log-normal grain size distribution deforming by diffusion creep at uniform strain rate $\dot{\epsilon}_{\dot{\epsilon}}^{\mathrm{diff}}$. When deformation occurs by pure dislocation creep, $\bar{\sigma}$ in Eq. (6b) is independent of grain size and is uniform in all grains, as described by Eq. (2). Rearranging Eq. (2) and using the definition of $B(T)$ given in Eq. (4), yields

$$\bar{\sigma}_{\dot{\epsilon}}^{\mathrm{disl}} = \left(\frac{\dot{\epsilon}_{\dot{\epsilon}}^{\mathrm{disl}}}{B(T)} \right)^{\frac{1}{n}} \quad (16)$$

for the volume averaged (uniform) stress when deformation occurs by dislocation creep at a homogeneous strain rate $\dot{\epsilon}_{\dot{\epsilon}}^{\mathrm{disl}}$. Rearranging Eqs. (15) and (16) to give $\dot{\epsilon}_{\dot{\epsilon}}$, putting $\bar{\sigma}_{\dot{\epsilon}}^{\mathrm{diff}} = \bar{\sigma}_{\dot{\epsilon}}^{\mathrm{disl}} = \bar{\sigma}_{\dot{\epsilon}}$ and summing now gives the following rough expression for the bulk creep rate of a polycrystalline material for the case that strain rate is homogeneously distributed in all grains:

$$\dot{\epsilon}_{\dot{\epsilon}}^{\mathrm{rough}} = \frac{A(T)}{(\exp[(3 + \frac{1}{2}m)\phi^2] r_{\mathrm{med}})^m} \bar{\sigma}_{\dot{\epsilon}} + B(T)\bar{\sigma}_{\dot{\epsilon}}^n \quad (17)$$

Note that the first term on the right here gives an expression for strain rate in terms of bulk stress, which is in fact a diffusion creep law for materials with a log-normally distributed grain size, assuming homogeneous strain rate (cf. Eq. (15)). This expression and the first term on the right of Eq. (13), which assumes homogeneous stress, give upper and lower bounds for the diffusion creep rate of materials with a log-normally distributed grain size. These expressions account for variations in standard deviation as well as median grain size and can be used in their own right to

describe or analyze the behavior of materials undergoing pure diffusion creep.

Eq. (17) closely approximates the exact relationship between bulk homogeneous strain rate $\dot{\epsilon}$ and bulk stress $\bar{\sigma}_{\dot{\epsilon}}$ only if one mechanism dominates. The true solution for $\dot{\epsilon}_{\dot{\epsilon}} = \dot{\epsilon}_{\dot{\epsilon}}(\bar{\sigma}_{\dot{\epsilon}})$ can be determined iteratively, by first determining $\bar{\sigma} = \sigma/\mu$ from Eq. (3) at fixed strain rate and fixed T, for a large range of realistic r-values. Subsequently, the integral in Eq. (6b) is evaluated by incrementally summing with respect to r, yielding $\bar{\sigma}_{\dot{\epsilon}}$. The whole operation is then repeated for different strain rates. The discrepancy or error in strain rate between the rough solution, given by Eq. (17), and the true strain rate ($\dot{\epsilon}_{\dot{\epsilon}}^{\text{true}}$) is defined here as

$$\Delta = \left(\frac{\dot{\epsilon}_{\dot{\epsilon}}^{\text{true}} - \dot{\epsilon}_{\dot{\epsilon}}^{\text{rough}}}{\dot{\epsilon}_{\dot{\epsilon}}^{\text{true}}} \right) \times 100\% \tag{18}$$

This error will be negligible towards low- and high-normalized stresses, where diffusion creep or dislocation creep, respectively, dominates, but large when both mechanisms contribute significantly to $\dot{\epsilon}_{\dot{\epsilon}}$. In addition, Δ will be small for small standard deviations, because the term $\exp[(3 + m/2)\phi^2]$ in Eq. (17) then approaches unity (single-valued grain size). The error Δ is dependent on all quantities appearing on the right hand side of Eq. (17), i.e. on $A(T)$, $B(T)$, r_{med}, ϕ, n, m and $\bar{\sigma}_{\dot{\epsilon}}$, but the error for a given material (fixed n, m, $A(T)$, $B(T)$) with constant grain size distribution (fixed r_{med}, ϕ) deforming at fixed conditions is only dependent on $\bar{\sigma}_{\dot{\epsilon}}$. The effects of $A(T)$, $B(T)$ and r_{med} can be removed by normalizing $\bar{\sigma}_{\dot{\epsilon}}$ with respect to $\bar{\sigma}_{\dot{\epsilon}}^{\text{int}}$, the normalized stress at the intersection between the diffusion and dislocation creep terms in Eq. (17) (i.e. the stress at which both terms contribute equally to the overall strain rate), using $\bar{\sigma}_{\dot{\epsilon}}^{*} = \bar{\sigma}_{\dot{\epsilon}}/\bar{\sigma}_{\dot{\epsilon}}^{\text{int}} = \bar{\sigma}_{\dot{\epsilon}}/\bar{\sigma}_{\dot{\epsilon}}^{\text{int}}$. When this is done, all curves of Δ versus $\bar{\sigma}_{\dot{\epsilon}}^{*}$ coincide for given n, ϕ and m, because the curves become independent of material parameters $A(T)$ and $B(T)$, temperature T and median grain radius r_{med}. The resulting Δ vs. $\bar{\sigma}_{\dot{\epsilon}}^{*}$ master-curve is roughly bell-shaped, peaking near $\bar{\sigma}_{\dot{\epsilon}}^{\text{int}}$. The function has been explored numerically by varying $\bar{\sigma}_{\dot{\epsilon}}^{*}$, n and ϕ through reasonable ranges, for both $m = 2$ and $m = 3$. This procedure showed (see results for $m = 3$ in Table 2) that Δ can be accurately approximated by the exponential distribution function

$$F(\bar{\sigma}_{\dot{\epsilon}}^{*}, \phi, n, m) = \exp\left(\alpha + \beta \bar{\sigma}_{\dot{\epsilon}}^{*0.5} \ln(\bar{\sigma}_{\dot{\epsilon}}^{*}) + \gamma \ln(\bar{\sigma}_{\dot{\epsilon}}^{*})^2\right) \tag{19}$$

in which α, β and γ are three independent parameters. Using this in the relation (cf. Eq. (18))

$$\dot{\epsilon}_{\dot{\epsilon}}^{\text{approx}} = \dot{\epsilon}_{\dot{\epsilon}}^{\text{rough}} \left(\frac{1}{1 - F(\bar{\sigma}_{\dot{\epsilon}}^{*}, \phi, n, m)} \right) \tag{20}$$

allows $\dot{\epsilon}_{\dot{\epsilon}}^{\text{true}}$ to be approximated by $\dot{\epsilon}_{\dot{\epsilon}}^{\text{approx}}$. This yields as a final result for the overall creep rate of a polycrystalline material with a log-normal grain size distribution, for the case that strain rate is uniform (i.e. constant) throughout the aggregate

$$\dot{\epsilon}_{\dot{\epsilon}}^{\text{approx}} = \left\{ \left[\frac{A_{\text{diff}} b D_{\text{diff}} \mu}{kT} \left(\frac{b}{\exp[(3 + \frac{1}{2}m)\phi^2] d_{\text{med}}} \right)^{m} \left(\frac{\sigma_{\dot{\epsilon}}}{\mu} \right) \right] + \left[\frac{A_{\text{disl}} b D_{\text{disl}} \mu}{kT} \left(\frac{\sigma_{\dot{\epsilon}}}{\mu} \right)^{n} \right] \right\} \left\{ \frac{1}{1 - F(\bar{\sigma}_{\dot{\epsilon}}^{*}, \phi, n, m)} \right\}$$

where

$$\bar{\sigma}_{\dot{\epsilon}}^{*} = \bar{\sigma}_{\dot{\epsilon}}/\bar{\sigma}_{\dot{\epsilon}}^{\text{int}} = \bar{\sigma}_{\dot{\epsilon}}/\bar{\sigma}_{\dot{\epsilon}}^{\text{int}}$$

with

$$\bar{\sigma}_{\dot{\epsilon}}^{\text{int}} = \left(\frac{A_{\text{diff}} D_{\text{diff}}}{A_{\text{disl}} D_{\text{disl}}} \right)^{\frac{1}{n-1}} \left(\frac{b}{\exp[(3 + \frac{1}{2}m)\phi^2] d_{\text{med}}} \right)^{\frac{m}{n-1}} \tag{21}$$

We further focus on Coble creep with $m = 3$ (cf. Karato et al., 1986). Values for the parameters α, β and γ for $m = 3$ are given in Table 3 (the entire range of $\bar{\sigma}_{\dot{\epsilon}}^{*}$ from pure diffusion creep to pure dislocation creep was covered in the numerical exploration, taking $3 \leq n \leq 5$ and $0 \leq \phi \leq 1.2$). Using these values for $m = 3$, $\dot{\epsilon}_{\dot{\epsilon}}^{\text{true}}$ is approximated by $\dot{\epsilon}_{\dot{\epsilon}}^{\text{approx}}$ within a factor of 0.9–1.1 for $n = 3$ and $\phi = 1.2$, and within 0.5–1.5 for $n = 5$ and $\phi = 1.2$, which is adequate for most purposes.

3. Discussion

We have derived constitutive equations describing composite diffusion plus dislocation creep for polycrystalline materials with a log-normally distributed grain size, assuming that either stress or strain rate is uniform throughout the aggregate. The two equations ((13) and (21)) allow investigation of the effect of varying grain size distribution on the rheology of materials deforming by these mechanisms. Note that the two equations represent upper and lower bounds for the rate of deformation in composite diffusion–dislocation creep of materials with a log-normal grain size distribution (Raj and Ghosh, 1981; Freeman and Ferguson, 1986; Tullis et al., 1991). We will now explore the differences between our composite flow laws and composite flow laws based on a single-valued grain size using polycrystalline olivine as an example. We focus attention on Coble creep and dislocation creep, for which the composition equation (21) has been fully explored. Finally, the implications for the rheology of other rock materials and for the application of flow laws to modeling and interpretation of natural rock deformation are discussed.

3.1. Universal deformation maps and the effect of grain size distribution on olivine

In order to make inferences about the effect of distributed grain size on the rheology of polycrystalline materials, the flow laws for a single-valued grain size (Eq. (3)) and a

Table 2
Expressions for parameters α, β and γ versus stress exponent n (quoted in table heading) with constants a and b used in the expression for each standard deviation ϕ. Parameters α, β and γ evaluated for $m = 3$ (Coble creep). With α, β and γ, the empirical function $F(\bar{\sigma}^*_{\dot{\epsilon}}, \phi, n, m)$, given by Eq. (19), can be used to reduce the error in strain rate to acceptable levels for deformation assuming homogeneous strain rate. The expressions can be used to estimate α, β and γ and determine $F(\bar{\sigma}^*_{\dot{\epsilon}}, \phi, n, m)$ for any stress exponent in the range $n = 3$–5 and any standard deviation in the range $\phi = 0$–1.2 by linear interpolation between the quoted values

Standard deviation	Expression $\alpha = (a + be^{-n})^{-1}$	Expression $\beta = a + bn$	Expression $\gamma = (a + b/n^2)^{-1}$
0.1	$a = -0.335$	$a = 1.13082$	$a = 0.2339$
	$b = 0.4619$	$b = -0.5664$	$b = -19.96$
0.2	$a = -0.581$	$a = 0.6056$	$a = 0.1760$
	$b = 1.203$	$b = -0.3515$	$b = -25.93$
0.3	$a = -0.919$	$a = 0.4155$	$a = 0.1316$
	$b = 2.434$	$b = -0.2459$	$b = -36.37$
0.4	$a = -1.41$	$a = 0.3025$	$a = 0.05871$
	$b = -4.499$	$b = -0.1780$	$b = -52.12$
0.5	$a = -2.14$	$a = 0.2256$	$a = -0.06970$
	$b = 8.046$	$b = -0.1305$	$b = -75.29$
0.6	$a = -3.28$	$a = 0.1697$	$a = -0.2600$
	$b = 14.29$	$b = -0.09589$	$b = -109.4$
0.7	$a = -5.12$	$a = 0.1279$	$a = -0.5423$
	$b = 25.50$	$b = -0.07032$	$b = -159.0$
0.8	$a = -8.18$	$a = 0.09565$	$a = -0.8690$
	$b = 45.96$	$b = -0.05110$	$b = -232.0$
0.9	$a = -13.5$	$a = 0.06933$	$a = -1.352$
	$b = 84.11$	$b = -0.03635$	$b = -336.0$
1.0	$a = -22.8$	$a = 0.05172$	$a = -1.333$
	$b = 155.7$	$b = -0.02595$	$b = -500.6$
1.1	$a = -39.5$	$a = 0.03773$	$a = -0.1743$
	$b = 285.9$	$b = -0.01821$	$b = -761.9$
1.2	$a = -69.4$	$a = 0.02767$	$a = 4.304$
	$b = 512.3$	$b = -0.01277$	$b = -1201$

log-normally distributed grain size assuming homogeneous stress (Eq. (13)) or homogeneous strain rate (Eq. (21)) are written in dimensionless form, i.e. in terms of normalized strain rate S. This yields

$$S = \left[C\left(\frac{\sigma}{\mu}\right) + \left(\frac{\sigma}{\mu}\right)^n \right]\left[\frac{1}{1 - F(\bar{\sigma}^*, \phi, n, m)} \right] \tag{22}$$

where

$$S = \frac{\dot{\epsilon} k T}{A_{\text{disl}} b D_{\text{disl}} \mu}$$

and

$$C = \frac{A_{\text{diff}} D_{0\text{diff}}}{A_{\text{disl}} D_{0\text{disl}}} \left(\frac{b}{X}\right)^m \exp\left(\frac{Q_{\text{disl}} - Q_{\text{diff}}}{RT}\right)$$

Here, $X = d$ and $F(\bar{\sigma}^*, \phi, n, m) = 0$ for a single-valued grain size (cf. Eq. (3)). For a log-normally distributed grain size and homogeneous stress (cf. Eq. (13)), $X = \exp[(3 - m/2)\phi^2)]d_{\text{med}}$ and $F(\bar{\sigma}^*, \phi, n, m) = 0$. For a log-normally distributed grain size, homogeneous strain rate and Coble creep (cf. Eq. (21)), $m = 3$, $X = \exp[(3 + m/2)\phi^2)]d_{\text{med}}$ and $F(\bar{\sigma}^*, \phi, n, m)$ is given by Eq. (19). With the dimensionless flow laws given in Eq. (22), universal deformation mechanism maps with pre-set C/n contours can be constructed in which dimensionless strain rate S is plotted versus dimensionless stress $\bar{\sigma}$. The advantage of these maps is that they apply to any single phase material in which grain size is spatially non-correlated, and any set of deformation conditions at which diffusion and dislocation creep are active. In one map, different materials and differences in deformation conditions or grain size (distribution) are represented by different C/n contours and can be investigated in the same map. In contrast, conventional maps (Frost and Ashby, 1982) apply to a single material with constant grain size, temperature, stress or strain rate, depending on the type of map (e.g. stress-temperature, grain size-stress, etc.).

In order to explore the differences between our composite flow laws and composite flow laws based on a single-valued grain size, we have constructed three universal deformation mechanism maps (Figs. 2–4). Fig. 2 shows a map for general materials with a single-valued grain size, constructed for different combinations of the power law stress exponents ($n = 3$, 4, 5) and values of the constitutive parameter C. Fig. 3 shows a map for materials with a log-normal grain size distribution, constructed for a power law stress exponent n of 3 or 5 and different values of C for homogeneous stress and strain rate. The C/n contours for homogeneous strain rate are drawn for standard deviations ϕ of 0, 0.5, 0.8 and 1.0. Fig. 4 shows a map for wet olivine with the log-normal grain size distributions as depicted in the inset ($d_{\text{med}} = 100$ μm, $\phi = 0$–1.2), deforming by Coble creep ($m = 3$) and power law dislocation creep ($n = 3$) at $T = 1273$ K. We used experimental data of Karato et al. (1986) for the rheology of wet olivine (Table 3) to construct this map, assuming this to apply for a single-valued grain size (though the data were of course derived from experiments on olivine rock with distributed grain size). Note that Karato et al. (1986) inferred deformation to occur by dislocation creep at high stress and Coble creep at low stress.

All maps have the following general characteristics. (1) The slope of individual curves (individual C/n contours) reflects the stress exponent of the dominant deformation mechanism. (2) All contours change in slope from n (the power law stress exponent) at high normalized stresses to one at low normalized stresses, reflecting dominant dislocation creep and diffusion creep, respectively. (3) With increasing temperature and (median) grain size C decreases (see Eq. (22)), so that at constant $\bar{\sigma}$ the normalized strain rate S will also decrease and power law dislocation creep will become increasingly important. In some cases a switch in deformation mechanism from diffusion to power law dislocation creep or vice versa can occur. The map of Fig. 2 can be used to illustrate examples of the effect of increasing temperature at constant grain size ($T = 1073$–1473 K, $d = 500$ μm, points 1–2 in Fig. 2) and increasing grain size at constant temperature ($d = 100$–500 μm,

Table 3
Constants and flow law parameters for Coble (A_{diff}, D_{0diff}, Q_{diff}) and dislocation (A_{disl}, D_{0disl}, Q_{disl}) creep in olivine from Karato et al. (1986) and Frost and Ashby (1982)

Parameter	Value	Dimensions	Remarks[a]
$A_{diff}\frac{\pi\delta}{b}D_{0diff}$	0.251	–	Calculated from rate constant quoted in Karato et al. (1986) and values from Frost and Ashby (1982)
$A_{disl}D_{0disl}$	2.80×10^{-4}	–	Calculated from rate constant quoted in Karato et al. (1986) and D_{0disl} value from Frost and Ashby (1982)
b	6.0×10^{-10}	m	Frost and Ashby (1982)
k	1.381×10^{-23}	J K^{-1}	
m	3	–	Karato et al. (1986)
n	3	–	Karato et al. (1986)
μ	7.10×10^{10}	Pa	For $T=1073$ K Temperature-dependent, data and equations from Frost and Ashby (1982) used
	6.83×10^{10}		For $T=1273$ K
	6.57×10^{10}		For $T=1473$ K
Q_{diff}	250,000	J mol^{-1}	Karato et al. (1986)
Q_{disl}	420,000	J mol^{-1}	Karato et al. (1986)
R	8.314	J mol^{-1} K^{-1}	

[a] Note that the data from Karato et al. (1986) are for grain boundary diffusion (Coble) creep and dislocation creep of wet hot-pressed San Carlos olivine and the data from Frost and Ashby (1982) are from various sources.

$T=1273$ K, points 3–4 in Fig. 2) for wet olivine with a single-valued grain size.

Note that the definition of the constitutive parameter C, given by Eq. (22), differs between the maps. The shape and position of the C/n contours for a single-valued grain size (Fig. 2) and for a distributed grain size assuming homogeneous stress (Figs. 3 and 4) are the same, because the second main term in Eq. (22) is unity in both cases. For a distributed grain size and assuming homogeneous strain rate, the shape of the C/n contours is determined by the function $F(\bar{\sigma}^{*}, \phi, n, m)$ (Fig. 3). The difference between the homogeneous stress (thick) and homogeneous strain rate (thin) contours increases with increasing distribution width ϕ, being largest at the mechanism transition where both diffusion and dislocation creep contribute significantly to the overall strain rate. When $\phi=0$, which is equivalent to a single-valued grain size, both stress and strain rate are distributed homogeneously throughout the material and the contours for homogeneous stress and strain rate coincide. For both homogeneous stress and homogeneous strain rate the volume fraction of grains deforming by dislocation creep increases with increasing ϕ for a given stress and d_{med}. This is accompanied by a decrease in C and S. For constant C and homogeneous strain rate, the range in $\bar{\sigma}$ covering the transition between diffusion and dislocation creep, changes from approximately one order of magnitude for small ϕ to more than five orders of magnitude for $\phi>1.0$ and $n=3$ (Fig. 3). Thus, when strain rate is homogeneous, the region where the two deformation mechanisms contribute significantly to the overall strain rate expands considerably in a material with distributed grain size.

We will now evaluate the effect of varying the standard deviation on the rheology of olivine rock with a distributed grain size using Fig. 4. As ϕ decreases from 1.2 to 0 (single-valued grain size), C increases from 3×10^{-9} for homogeneous stress or 7×10^{-15} for homogeneous strain rate to 2×10^{-6}. For olivine deforming at a normalized stress of 7.4×10^{-5} (~5 MPa), this means that S increases by more than two orders of magnitude from 6×10^{-13} (homogeneous stress) or 4×10^{-13} (homogeneous strain rate) to 1×10^{-10}, equivalent to an increase in absolute strain rate of more than two orders of magnitude from 2×10^{-12} to 5×10^{-10} s^{-1}. In addition, a switch in rheological behavior from dominantly dislocation to dominantly Coble creep occurs, as shown at 5 MPa in Fig. 4. Fig. 5 illustrates the effect of decreasing ϕ on absolute strain rate (in s^{-1}) for olivine deforming at ~5 MPa and 1273 K in detail. The increase in strain rate is even greater towards lower stresses, but decreases towards higher stresses where grain size insensitive dislocation creep becomes more important.

The above example for olivine (Figs. 4 and 5) demonstrates a substantial change in strain rate of wet polycrystalline olivine (with fixed d_{med}) deforming at a given stress if the width of the grain size distribution changes. Conventional flow laws that regard grain size as single-valued do not account for this effect and would predict strain rates similar to the strain rate at $\phi=0$ for the entire range in ϕ (Fig. 5). It should be noted, however, that the flow parameters of olivine used (Table 3) are determined for olivine with a specific (unreported) grain size distribution, but fitted to a flow law for a single-valued grain size (Karato et al., 1986). Strictly then, these parameters should not be used in flow laws for a distributed grain size. Rather, true flow law parameters should be determined independently by fitting flow laws for distributed grain size to mechanical data obtained for materials with a known grain size distribution. Only then can the absolute changes in $\dot{\epsilon}$ related to a change in ϕ be accurately evaluated. The present

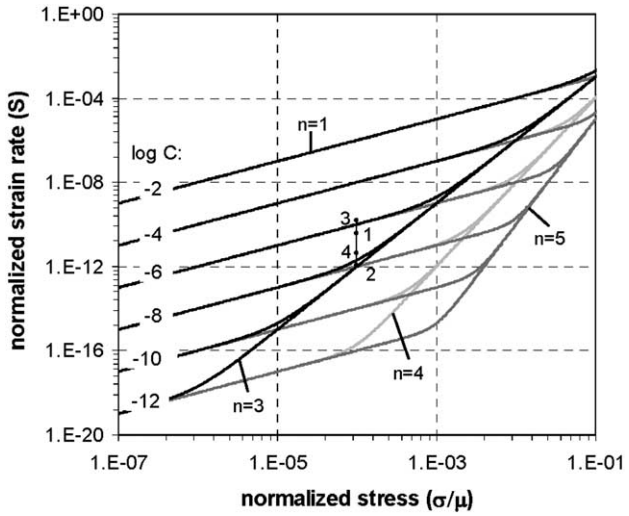

Fig. 2. Universal deformation mechanism map for materials with a single-valued grain size, deforming by combined diffusion and power law dislocation creep. The map shows contours of $C = \frac{A_{\mathrm{diff}} D_{0\mathrm{diff}}}{A_{\mathrm{disl}} D_{0\mathrm{disl}}} \left(\frac{b}{d}\right)^m \exp\left(\frac{Q_{\mathrm{disl}} - Q_{\mathrm{diff}}}{RT}\right)$ in logarithmic space of normalized (dimensionless) strain rate $S = \frac{\dot{\epsilon} kT}{A_{\mathrm{disl}} b D_{\mathrm{disl}} \mu}$ versus normalized (dimensionless) stress for a power law stress exponent n of 3, 4 or 5. The slope of the contours reflects n. Points $1 \rightarrow 2$ show the effect of changing temperature ($T = 1073 \rightarrow 1473$ K) at constant grain size ($d = 500$ μm) and points 3–4 show the effect of changing grain size ($d = 100 \rightarrow 500$ μm) at constant temperature ($T = 1273$ K) for olivine deforming by dislocation and Coble creep (Karato et al., 1986) at a normalized stress of 1×10^{-4}.

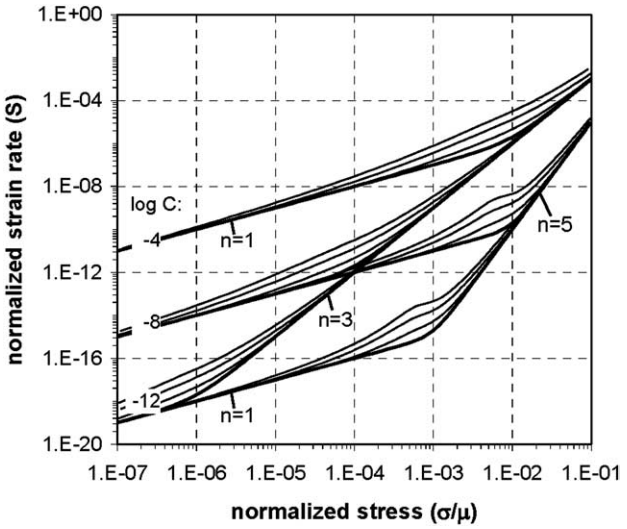

Fig. 3. Universal deformation mechanism map for materials with a distributed grain size, deforming by combined Coble and power law dislocation creep. The map shows contours of $C = \frac{A_{\mathrm{diff}} D_{0\mathrm{diff}}}{A_{\mathrm{disl}} D_{0\mathrm{disl}}} \left(\frac{b}{X}\right)^m \exp\left(\frac{Q_{\mathrm{disl}} - Q_{\mathrm{diff}}}{RT}\right)$, with $X = \exp[(3 - m/2)\phi^2)] d_{\mathrm{med}}$ for homogeneous stress and $X = \exp[(3 + m/2)\phi^2)] d_{\mathrm{med}}$ for homogeneous strain rate, in log normalized strain rate $S = \frac{\dot{\epsilon} kT}{A_{\mathrm{disl}} b D_{\mathrm{disl}} \mu}$ versus log normalized stress $\bar{\sigma}$ space for material with a log-normal grain size distribution and a power law stress exponent n of 3 or 5. The slope of the contours reflects n. The contours for homogeneous stress are represented by thick lines. Those for homogeneous strain rate are represented by thin lines, corresponding to standard deviations ϕ of 0.5, 0.8 and 1.0 (from bottom to top for each set of contours). The irregularity in the homogeneous strain rate contours for $n = 5$ is due to the residual error in strain rate, which is highest for the largest stress exponent and standard deviation. Note that all strain rates for $n = 3$–5 and $\phi = 0$–1.2 are accurate within a factor of two or better.

example (Figs. 4 and 5) nonetheless illustrates that variation in standard deviation can have a major effect on the rheology of materials such as olivine.

3.2. Implications for the rheology of rock materials in general

We now address the question of what the general implications of the present model are for the rheology of materials in nature and experiment. From the foregoing, it is evident that three inter-related points need consideration:

(1) The calibration of flow laws using laboratory data. Mechanical data obtained from laboratory deformation experiments are often fitted to single mechanism flow laws, incorporating a single-valued grain size (Frost and Ashby, 1982). The present analysis shows that in many cases grain size distributions consist of small grains deforming by GSS deformation mechanisms and large grains deforming by GSI deformation mechanisms. In addition, the transition zone between both GSS and GSI mechanisms may spread out over several orders of magnitude in stress (cf. Fig. 3). Apparent flow law parameters, such as stress exponents, are often obtained by fitting mechanical data collected in the transition zone to conventional flow laws (single mechanism, single-valued grain size) and given mechanistic significance. However, the resulting values will not be representative of the deformation mechanisms operating. Instead, the apparent flow law parameters will reflect intermediate values of the true parameters associated with the individual active deformation mechanisms. This problem is particularly apparent if multiple (more than two) GSS and GSI deformation mechanisms operate, producing multiple transition zones that interact to yield apparent flow law parameters reflecting the interplay of a series of deformation mechanisms.

(2) Interpretation of microstructures in terms of deformation mechanisms. Part of the justification of applying flow laws to nature comes from the comparison of microstructures between nature and experiment. If grain size is distributed, different grains may deform by different deformation mechanisms. The most easily observed mechanism may accordingly not be most important in controlling flow and is definitely not exclusively responsible for deformation. By applying conventional flow laws, determined empirically from an apparently dominant (single) deformation mechanism and single-valued grain size, the contribution of other potentially important deformation mechanisms is disregarded.

(3) Application of flow laws to natural rocks. When

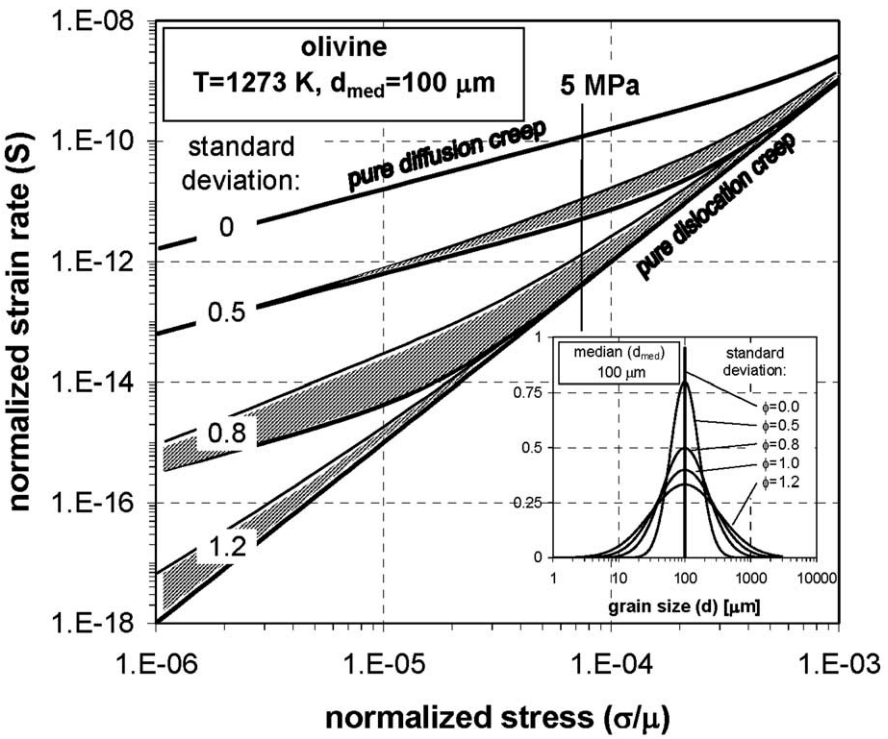

Fig. 4. Deformation map for wet olivine, deforming by Coble creep and power law dislocation creep described by the parameters listed in Table 3 (Karato et al., 1986). The map shows contours of C in log normalized strain rate S versus log normalized stress space, assuming a log-normal grain size distribution having a fixed median and varying standard deviation, as depicted in the inset. Values of C vary from 1.6×10^{-6} for $\phi = 0$ to 6.6×10^{-15} for $\phi = 1.2$. For each standard deviation ϕ, the true normalized strain rate S falls between the homogeneous stress (lower thick lines) and the homogeneous strain rate (upper thin lines) bounds (shaded area). For $T = 1273$ K, the normalized stress equivalent to 5 MPa is indicated.

conventional flow laws are applied to evaluate flow in natural rocks, differences in grain size distribution are not taken into account. However, grain size distributions in naturally deformed rocks show a wide range of standard deviations ($\phi = 0.7–1.0$ for ln$d$, estimated from grain size distributions reported in Michibayashi (1993) for quartz in diorites, metasediments and granites; Newman (1994) for calcite in mylonites; Molli et al. (2000) for calcite in marble; Dijkstra et al. (2002) for olivine in dunites).

This study reveals that disregarding differences in standard deviation between the natural rock under investigation and the material used for calibration of the flow law may be significantly over- or underestimating stresses and strain rates in nature. This effect is illustrated in Fig. 6 for the example of wet olivine with $d_{\text{med}} = 100$ μm, deforming by Coble creep ($m = 3$) plus dislocation creep at $\sigma = 5$ MPa and $T = 1273$ K (cf. Fig. 5). To construct Fig. 6, the full grain size distribution of wet San Carlos olivine used in the study by Karato et al. (1986) was analyzed from the micrograph they presented (Karato et al., 1986; Fig. 3a). Further, the pre-exponential rate constant A_{diff} (cf. Table 3) was adjusted to account for the standard deviation of this grain size distribution (following Eqs. (13) and (21) for homogeneous stress and strain rate, respectively). Then, the ratio $\dot{\epsilon}_2/\dot{\epsilon}_1$

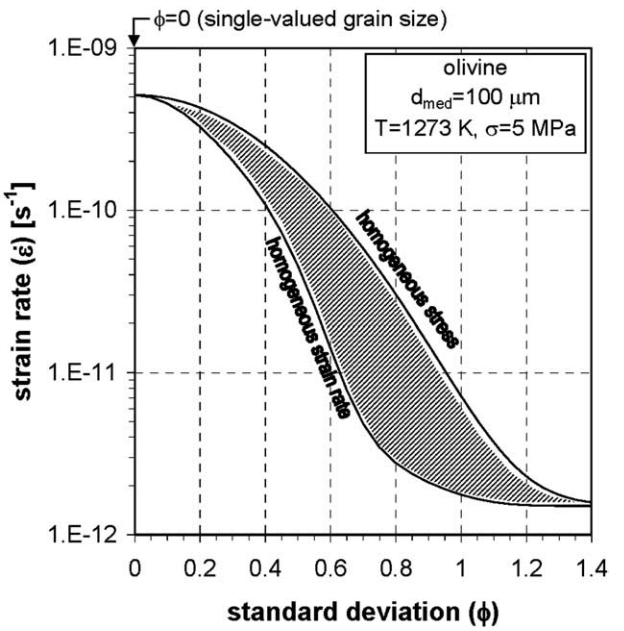

Fig. 5. Variation of absolute strain rate $\dot{\epsilon}$ (s^{-1}) with standard deviation of the log-normal grain size distribution ϕ for wet olivine deforming at $T = 1273$ K and $\sigma = 5$ MPa. The true strain rate falls in between the homogeneous stress (upper line) and homogeneous strain rate (lower line) bounds (shaded area). Flow law parameters used for olivine are from Karato et al. (1986) (Table 3).

between the strain rate ($\dot{\epsilon}_2$) of the olivine rock samples used in the laboratory (with standard deviation ϕ_2) and the strain rate ($\dot{\epsilon}_1$) of natural olivine rock (with standard deviation ϕ_1) was calculated for the specified natural deformation conditions and plotted (Fig. 6). The ratio $\dot{\epsilon}_2/\dot{\epsilon}_1$ therefore depicts the amount by which the strain rate of the natural rock is overestimated (for $\phi_1 > \phi_2$) or underestimated (for $\phi_1 < \phi_2$) if the standard deviation of the grain size distribution is unaccounted for. Fig. 6 emphasizes that conventional single grain size flow laws significantly over- or underestimate strain rates, because ϕ_1 and ϕ_2 are assumed equal regardless of actual differences in standard deviation between the natural and laboratory olivine rock (i.e. $\phi_1 \neq \phi_2$). As an example of over- or underestimation of strain rate in natural rocks, the standard deviation of the grain size distribution exhibited by the olivine rock material used in the study by Karato et al. (1986) (line A), together with some realistic values of standard deviations from upper mantle dunites of the Oman ophiolite analyzed by Dijkstra et al. (2002) (lines B and C) are included in the diagram. Fig. 6 shows that for the chosen combination of deformation conditions, median grain size and standard deviations, the strain rate in the natural rock may be overestimated by a factor ~10–50 or ~200–300 ($\dot{\epsilon}_2/\dot{\epsilon}_1$ ratio at intersection of line A with lines B and C) for homogeneous stress or strain rate, respectively, due to differences in standard deviation alone. Evidently, this effect will be even larger for rocks or conditions where GSS deformation is more important (e.g. in peridotite mylonites; Jaroslow et al., 1996) and will be smaller for rocks or conditions where GSI deformation is more important (e.g. in coarse porphyroclastic peridotite; Nicolas et al., 1980).

The three points mentioned above illustrate the problems associated with the application of conventional single mechanism flow laws based on a single-valued grain size. Although we do not claim that the flow laws presented in the present paper solve the problems associated with extrapolating laboratory data to nature, they offer better constraints on stress and strain rate in nature, due to the improvements made concerning multiple deformation mechanisms and incorporation of grain size distribution. Accordingly, the flow laws can help to improve geodynamic models that use flow laws to describe the rheology of rock materials.

In their present form, the flow laws describe the rheology of single-phase materials with spatially non-correlated, log-normally distributed grain size undergoing steady-state deformation by a combination of diffusion and dislocation creep. However, as mentioned before, the derivation can be applied to other or more deformation mechanisms or other grain size distributions as well, that is as long as the deformation mechanisms operate independently and the integrals containing the specific probability density function describing the grain size distribution can be solved. The flow laws are also important in modeling of more complex rocks, for example with multiple phases or with interconnected layering or load bearing frameworks of specific grain size (cf. Handy, 1990), because the different layers or phases will consist of material with a specific grain size distribution that need to be accounted for. The flow laws also offer a starting point for models that describe non-steady state deformation caused by microstructural evolution resulting from processes such as dynamic recrystallization. Incorporation of (the evolution of) grain size distributions will be a crucial element of such models.

4. Summary and conclusions

1. Constitutive flow equations describing deformation of materials generally are grain size insensitive (dislocation creep) or include grain size as a single value (e.g. diffusion creep). However, materials invariably exhibit a grain size distribution, implying that in the same aggregate small grains may deform by a different mechanism than large grains.

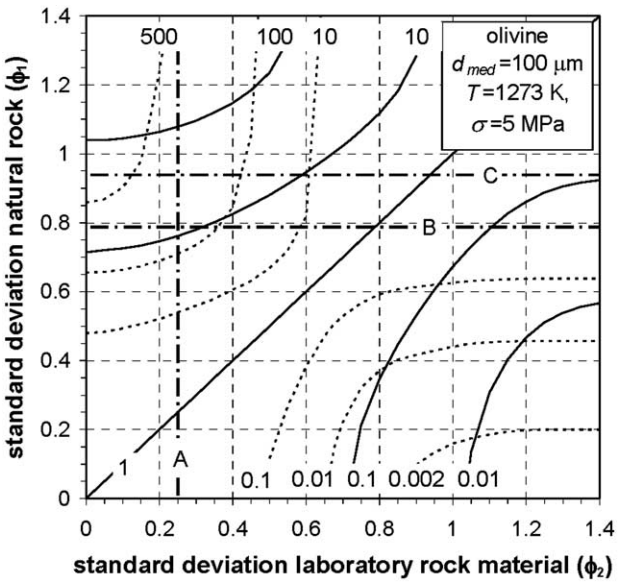

Fig. 6. Variation in strain rate (expressed as the ratio $\dot{\epsilon}_2/\dot{\epsilon}_1$) due to differences in standard deviation between the olivine rock in nature (with ϕ_1) and the olivine rock material used in the laboratory to calibrate the flow law (with ϕ_2). $\dot{\epsilon}_1$ represents the strain rate of the natural rock and $\dot{\epsilon}_2$ the strain rate of the laboratory material at similar deformation conditions. In this example, we have taken $T = 1273$ K and $\sigma = 5$ MPa for the deformation conditions and $d_{med} = 100$ μm for the median grain size (cf. Fig. 5). The standard deviation of the olivine rock material used in the study by Karato et al. (1986) (line A) and two standard deviations of dunites from the Oman ophiolite analyzed by Dijkstra et al. (2002) (lines B and C) are indicated. A flow law for a single-valued grain size cannot account for variations in ϕ and therefore may overestimate the strain rate by a factor ~10–50 ($\dot{\epsilon}_2/\dot{\epsilon}_1 = 10$–50) for homogeneous stress or by a factor ~200–300 ($\dot{\epsilon}_2/\dot{\epsilon}_1 = 200$–300) for homogeneous strain rate in this example (intersection line A with lines B and C).

2. We have derived theoretical composite diffusion-dislocation creep laws for materials with a continuous log-normal grain size distribution under the assumption that either stress or strain rate is uniform in the material. The flow laws describe lower and upper bounds for the rate of deformation in materials with a distributed grain size and allow systematic investigation of the effect of varying the grain size distribution on rheology. In the flow laws, grain size distribution is characterized by the median grain size and standard deviation.
3. Composite flow laws that incorporate parameters characterizing the grain size distribution provide better constraints on rheology and the interpretation of active deformation mechanisms in natural rocks, thereby helping to improve geodynamic models. This is due to the following aspects:
   (a) Difficulties with the interpretation of apparent (intermediate) values for flow parameters resulting from fitting experimental data to empirical single mechanism, single-valued grain size flow laws in cases where multiple mechanisms are active can be largely avoided.
   (b) Interpretation of active deformation mechanisms using mechanical and microstructural data can be improved, because all active mechanisms, not only the apparent dominant one, are accounted for.
   (c) Extrapolation of experimentally calibrated flow laws to nature can be done more reliably, because differences between the grain size distribution of naturally deformed rocks and that of the materials tested in the laboratory can be accounted for.
4. After expressing the flow laws in dimensionless form, universal deformation mechanism maps can be constructed that apply to any single phase material in which grain size is spatially non-correlated, and to any set of realistic deformation conditions at which diffusion and dislocation creep operate. A single map can then be used to compare deformation characteristics of different single phase materials and grain size distributions.
5. Whereas the flow law for uniform stress is routinely applicable in a manner similar to conventional flow laws, routine application of the flow law for uniform strain rate requires an approximation in which parameters for a single diffusion creep mechanism are used. We focused in this paper on the application of the flow laws to olivine, deforming by a combination of dislocation and Coble creep. This showed that for a realistic range of standard deviations ($\phi = 0$–1.2), the strain rate can change by orders of magnitude with increasing standard deviation. In some cases even a switch in rheological behavior from dominant Coble creep to dominant dislocation creep or vice versa can be induced. Conventional flow laws based on a single-valued grain size therefore may significantly over- or underestimate strain rates or stresses in nature if the grain size distribution of the natural rock differs from that of the material used in laboratory experiments to calibrate the flow law.

Acknowledgements

The manuscript benefited from discussions with M.R. Drury and B. Bos. We gratefully acknowledge constructive comments by referees G. Ranalli and R. Heilbronner.

References

Aitchison, J., Brown, J.A.C., 1957. The Lognormal Distribution, with Special Reference to its use in Economics, Cambridge University Press, Cambridge.

Ashby, M.F., Verall, R.A., 1973. Diffusion-accommodated flow and superplasticity. Acta Metallurgica 21, 149–163.

Coble, R.L., 1963. A model for boundary diffusion controlled creep in polycrystalline materials. Journal of Applied Physics 34, 1679–1682.

Dijkstra, A.H., Drury, M.R., Frijhoff, R., 2002. Microstructures and lattice fabrics in the Hilti mantle section (Oman Ophiolite): evidence for shear localization and melt weakening in the crust-mantle transition zone? Journal of Geophysical Research 107, 2270, DOI: 10.1029/2001JB000458.

Freeman, B., Ferguson, C.C., 1986. Deformation mechanism maps and micromechanics of rocks with distributed grain sizes. Journal of Geophysical Research 91, 3849–3860.

Frost, H.J., Ashby, M.F., 1982. Deformation–Mechanism Maps: the Plasticity and Creep of Metals and Ceramics, Pergamon Press, Oxford.

Gradshteyn, I.S., Ryzhik, I.M., 1980. Table of Integrals, Series and Products, Academic Press, San Diego.

Handy, M.R., 1990. The solid-state flow of polymineralic rocks. Journal of Geophysical Research 95, 8647–8661.

Hashin, Z., 1964. Theory of mechanical behavior of heterogeneous media. Applied Mechanics Reviews 17, 1–9.

Heilbronner, R., Bruhn, D., 1998. The influence of three-dimensional grain size on the rheology of polyphase rocks. Journal of Structural Geology 20, 695–705.

Herring, C., 1950. Diffusional viscosity of a polycrystalline solid. Journal of Applied Physics 21, 437–445.

Hill, R., 1965. A self-consistent mechanics of composite materials. Journal of the Mechanics and Physics of Solids 13, 213–222.

Humphreys, F.J., Hatherly, M., 1996. Recrystallization and Related Annealing Phenomena, Pergamon Press, Oxford.

Jaroslow, G.E., Hirth, G., Dick, H.J.B., 1996. Abyssal peridotite mylonites: implications for grain-size sensitive flow and strain localization in the oceanic lithosphere. Tectonophysics 256, 17–37.

Karato, S., Paterson, M.S., FitzGerald, J.D., 1986. Rheology of synthetic olivine aggregates: influence of grain size and water. Journal of Geophysical Research 91, 8151–8176.

Kohlstedt, D.L., Evans, B., Mackwell, S.J., 1995. Strength of the lithosphere: constraints imposed by laboratory experiments. Journal of Geophysical Research 100, 17587–17602.

Kretz, R., 1966. Grain size distribution for certain metamorphic minerals in relation to nucleation and growth. Journal of Geology 74, 147–173.

Michibayashi, K., 1993. Syntectonic development of a strain-independent steady-state grain size during mylonitization. Tectonophysics 222, 151–164.

Miralles, L., Sans, M., Pueyo, J.J., Santanach, P., 2000. Recrystallization

salt fabric in a shear zone (Cardona diapir, southern Pyrenees, Spain). In: Vendeville, B., Mart, Y., Vigneresse, J.-L. (Eds.), Salt, Shale and Igneous Diapirs in and around Europe. Geological Society Special Publication 174, pp. 149–167.

Molli, G., Conti, P., Giorgetti, G., Meccheri, M., Oesterling, N., 2000. Microfabric study on the deformational and thermal history of the Alpi Apuane marbles (Carrara marbles), Italy. Journal of Structural Geology 22, 1809–1825.

Mukherjee, A.K., 1975. High-temperature creep. In: Arsenault, R.J. (Ed.), Treatise on Material Science and Technology 6, pp. 163–224.

Nabarro, F.R.N., 1948. Report of a Conference on Strength of Solids, The Physical Society, Bristol, pp. 75–90.

Newman, J., 1994. The influence of grain size and grain size distribution on methods for estimating paleostresses from twinning in carbonates. Journal of Structural Geology 16, 1589–1601.

Nicolas, A., Boudier, F., Boucher, J.-L., 1980. Interpretation of peridotite structures from ophiolitic and oceanic environments. American Journal of Science 280, 192–210.

Poirier, J.P., 1985. Creep of Crystals—High-temperature Deformation Processes in Metals, Ceramics and Minerals, Cambridge University Press, Cambridge.

Post, A., Tullis, J., 1999. A recrystallized grain size piezometer for experimentally deformed feldspar aggregates. Tectonophysics 303, 159–173.

Raj, R., Ghosh, A.K., 1981. Micromechanical modelling of creep using distributed parameters. Acta Metallurgica 29, 283–292.

Ranalli, G., 1984. Grain size distribution and flow stress in tectonites. Journal of Structural Geology 6, 443–447.

Rutter, E.H., Brodie, K.H., 1988. The role of tectonic grain size reduction in the rheological stratification of the lithosphere. Geologische Rundschau 77, 295–308.

Schückher, F., 1968. Grain size. In: DeHoff, R.T., Rhines, F.N. (Eds.), Quantitative Microscopy, McGraw-Hill Series in Materials Science and Engineering, pp. 201–265.

Tsenn, M.C., Carter, N.L., 1987. Upper limits of power law creep of rocks. Tectonophysics 136, 1–26.

Tullis, T.E., Horowitz, F.G., Tullis, J., 1991. Flow laws of polyphase aggregates from end-member flow laws. Journal of Geophysical Research 96, 8081–8096.

Wang, J.N., 1994. The effect of grain size distribution on the rheological behavior of polycrystalline materials. Journal of Structural Geology 16, 961–970.

Weertman, J., 1968. Dislocation climb theory of steady-state creep. Transactions of the American Society for Metals 61, 681–694.